PHOTOCURRENT MEASUREMENTS OF THE PURPLE MEMBRANE ORIENTED IN A POLYACRYLAMIDE GEL

S. Y. Liu and T. G. Ebrey
University of Illinois, Department of Physiology and Biophysics, Urbana, Illinois 61801

ABSTRACT When illuminated, oriented purple membranes isolated from *Halobacterium halobium* give a photoelectric effect. The frequency response of a photocurrent measuring system for purple membranes oriented and immobilized in a polyacrylamide gel is analyzed from DC to 100 MHz. The waveform of the photocurrent can depend on both the sample conditions (including bathing solution) and the measuring system (electrode and ammeter) at both the low and high frequency ends. In the DC – 1 kHz range (millisecond signals), the apparent lifetime of the photocurrent component is distorted if the electrode is not platinized and if the conductivity of the bathing solution is not low. In the 1 kHz to 1 MHz range (microsecond signals), the frequency response is flat under most conditions. In the MHz range (nanosecond signals), the apparent lifetime of the photocurrent component will be distorted if the conductivity of the bathing solution is not high and if the input impedance of the ammeter is not low and constant throughout the frequency range. With our optimized apparatus, we could measure the photocurrent components from oriented purple membrane with lifetimes from 70 ms to 32 ns without distortion by the measuring system.

INTRODUCTION

Oriented purple membranes of *Halobacterium halobium* produce an electrical signal when irradiated. This photoelectric response is probably due to internal charge movements associated with light-induced conformational changes of the bacteriorhodopsin and external charge movements such as proton pumping and ion release from the purple membrane (for reviews see Keszthelyi, 1984; Trissl, 1985).

The photoelectric signal of bacteriohodopsin has at least three components with different lifetimes in the picosecond to millisecond range: (*a*) A fast component in the direction opposite to that of physiological proton translocation with a rise time <100 ps (Groma, et al., 1984; Trissl, 1985); For convenience, we call this component the first negative component since we define the direction that the proton is transferred as positive. This component is believed to be associated with the formation of the K intermediate of the bacteriorhodopsin photocycle and the charge movement induced by all-*trans* to 13-*cis* isomerization of retinal may be the direct source of the signal (Keszthelyi et al. 1983; Trissl et al. 1987). Liu et al. (1987) have shown that a modified all-*trans* retinal which cannot isomerize to 13-*cis* retinal does not have this component. (*b*) A positive component with a lifetime of ~40 μs. This component correlates fairly well with the L-M spectral transition. Whether this photoelectric signal is due to internal charge movement or proton release on the surface of purple membrane is not clear. (*c*) A slower positive component with a lifetime in the millisecond range with an amplitude much smaller than the faster components. Sometimes this component has the same kinetics as the M intermediate (e.g., at normal pH and moderate ionic strength, Ormos et al., 1985). The origin of this component is also not clear. It could be due to internal charge movement of purple membrane or the release or uptake of protons or other ions on the surface of purple membrane.

Two classes of methods have been used to detect the photoelectric signals: (*a*) photovoltage measurements, sometimes referred as open circuit measurements, and (*b*) photocurrent or short circuit measurements. Theoretically, from a photocurrent measurement we can get the photovoltage and vice versa. In practice, the relationship of photovoltage and photocurrent is very complicated because ideal open or short circuit conditions are not easily achievable. Often a measuring system is used which makes measurements close to open circuit conditions over one frequency range but close to short circuit conditions over another frequency range.

The various advantages and disadvantages of photovoltage versus photocurrent measurements are controversial. Generally speaking, photovoltage measurements are good for the study of very fast kinetics. They are less sensitive to the parameters of the sample and measuring system such as ionic strength and amplifier impedance. Moreover, the instrumentation for photovoltage measurements is comparably easier to make and the high speed, low noise amplifier needed is also easier to obtain commercially. Photovoltage responses with a time resolution up to 100 ps have been detected (Groma et al., 1984; Trissl, 1985). However, if using the quite advantageous electric field oriented sample (see below), photovoltage measurements of long lifetime photoelectric events are difficult, while

photocurrent measurements are limited only for very fast signals (see below). Moreover, photocurrent measurements can easily be used to study quantitatively the kinetics of the internal charge movement of bacteriorhodopsin, since the amplitude of displacement current directly reflects the number and distance charges move in the purple membrane, and the kinetics of the photocurrent is related to the kinetics of the bacteriorhodopsin's photointermediates (Fahr et al., 1981). Therefore, we have chosen to measure the photocurrent.

There are several technical problems for photocurrent measurements. Because an ammeter cannot be directly connected to the purple membrane but must be connected via an intermediate such as an electrolyte solution which has a nonzero resistance, an ideal short circuit current measurement cannot be achieved. Another problem is that a high speed, high gain, low noise and low input impedance ammeter is more difficult to construct and handle than the corresponding voltmeter. However, under restricted conditions and frequency ranges the displacement current of the purple membrane will be in phase with the current going through the ammeter and has a simple linear relationship to it. Moreover, recent developments have greatly improved the ease of building the required circuits for photocurrent measurements. For bulk purple membrane sheets oriented in an electric field a flat frequency range for photocurrent measurements in the 1 ms to 1 μs time range can be easily achieved under most conditions (see below), allowing a *de facto* photocurrent measurement. Further extending this flat frequency range is possible and will be discussed in this report.

Two types of preparations have been developed to orient the purple membrane for studies of their photoelectric activity (Trissl, 1985). (*a*) A thin layer of purple membrane is oriented at an interface. For example, purple membrane is absorbed onto a planar lipid bilayer (Fahr et al., 1981); a thin Teflon film (Trissl et al., 1977), a heptane/water interface (Trissl, 1983), or a lipid-impregnated filter (Drachev et al., 1978; Herrmann et al., 1978). (*b*) Purple membrane sheets are oriented in a electric field either transiently in a low ionic strength solution (Keszthelyi et al., 1980), or permanently by being immobilized in a polyacrylamide gel (Dér et al., 1985), or dried on a conductive glass (Váró, 1981). The electric field oriented sample system has a major advantage in that the absorbance of the sample is large enough so that optical as well as electrical measurements can be made simultaneously (see also Trissl, 1985). For this reason we have chosen to work with electric field oriented samples.

The method of immobilizing oriented purple membrane in a polyacrylamide gel is a particularly convenient method for studies of the kinetics of the photocurrent, because one is able to change ionic strength and pH while maintaining constant orientation of purple membrane sheets. However, understanding the relationship of measurement system (including salt solution, electrodes, and amplifier) to the signal is important for kinetic studies and will help avoid some potential artifacts of the measuring system.

Here we present a frequency analysis of a polyacrylamide gel sample/photocurrent measuring system in the DC to 100 MHz range. We have developed optimized conditions so that we can measure the kinetics of the photocurrent from 70 ms to 32 ns without the shape of the signal being distorted by the measuring system.

MATERIALS AND EQUIPMENT

Purple membrane was prepared from *Halobacterium halobium* strain S-9 cells according to the method of Becher and Cassim (1975), except that the DNase treatment was omitted.

Oriented purple membranes (90 μM) were immobilized in a polyacrylamide gel by the method of Dér et al. (1985) (except that the final concentration of ammonium persulfate is 0.25%). A piece of the gel was cut to 5 × 5 × 10 mm and put in a 5 × 10 × 45 mm cuvette with two platinum wire electrodes 8 mm apart on each side of the gel. The gel was washed in distilled water for 24 h then bathed in a KCl solution of the required ionic strength for ~1 h before the measurement.

The sample was excited by a frequency-doubled Nd-YAG laser (λ = 532 nm) with 7 ns pulse width. The photocurrent signal was measured with a current to voltage converter (I-V converter). After the signals went through the I-V converter, they were sent to an attenuator (406A 0-1 GHz, 0-130 dB; Kay Elemetrics Corp., Pine Brook, N.J.), then to a homemade voltage amplifier with DC to 100 MHz bandwidth, and finally, recorded by a LeCroy 8837 digitizer (32 MHz sampling frequency, DC to 100 MHz bandwidth; LeGroy Research Systems Corp., Spring Valley, NY). The optical measurements were done as described by Dancsházy et al. (1986).

Impedance measurements in the 400 KHz-100 MHz range were done with a Hewlett-Packard 4193A vector impedance meter (Hewlett-Packard Co., Palo Alto, CA). The probing currents was 100 μA. For the 5–100 KHz range, the impedance was measured with an EG&G electrochemical impedance system model 378 (Princeton Applied Research, Princeton, NJ). The probing voltage was 5 mV.

The input impedances of the I-V converters constructed with the operational amplifiers (op-amp) were measured by inputting a sine wave current (1 μA) to the I-V converter which has had its input terminals shunted with a resistor. The resistor was adjusted until the output voltage was one half of the output without the resistor; at this point the resistor's value was equal to the input resistance.

The electrodes initially tested, two smooth surface platinum wires 1 mm in diameter and 8 mm apart, were connected with twisted wire to the I-V converter; the total length from the tip of the electrodes to the I-V converter was 15 cm.

CIRCUIT ANALYSIS AND MEASUREMENT SYSTEM

1. Description

Fig. 1 *a* shows a schematic diagram of the measuring system including the gel, salt solution, electrodes, and I-V converter. All the electronic elements that could affect the photocurrent are drawn in. In order to determine the frequency response of the system the value of each circuit element must be determined. For ease to analyze, the circuit in Fig. 1 *a* is redrawn in Fig. 1 *b*.

I_s is a current source representing the purple membrane. It is proportional to the number of bacteriorhodopsins excited by the laser and the distance that the charges move. I_0 is the photocurrent through the I-V converter.

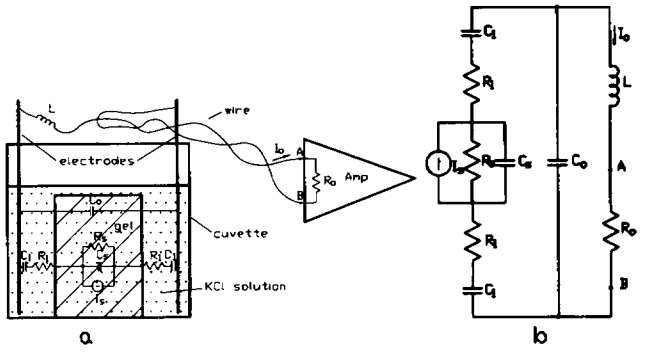

FIGURE 1. (*a*) Schematic diagram of the measuring system and its equivalent circuit. All the electronic elements that will affect the photocurrent are drawn in. I_s is the current source, I_o is the current through the I-V converter, R_s is the source resistance, C_s is the source capacitance, R_l is the electrolyte solution's resistance, C_l is the double layer capacitor between electrolyte and electrode, C_o is the capacitance between two electrodes, L is the inductance of the wires, and the R_o is the input impedance of the I-V converter. See text for details. (*b*) The circuit in *a* redrawn.

L is the inductance of the electrodes and the wire connecting them to the I-V converter. C_o is the value of the capacitance parallel to R_o. It includes the stray capacitance between the two electrodes and their wires but is mostly due to the part of electrodes that are immersed in the electrolyte solution. R_l is the resistor connecting the membranes in the gel to the electrode. The resistance is determined by the type and concentration of the electrolyte solution bathing the gel. The values of L, R_l, and C_o are determined by replacing the I-V converter at points A and B and measuring the impedance from 400 KHz to 100 MHz. In this frequency range the remaining part of circuit, as drawn in Fig. 2 *a*, can be reduced to Fig. 2 *b* since both R_s (few Ω) and C_l (μF range) could be looked on as shorts. Fitting the Bode amplitude and Bode phase plots

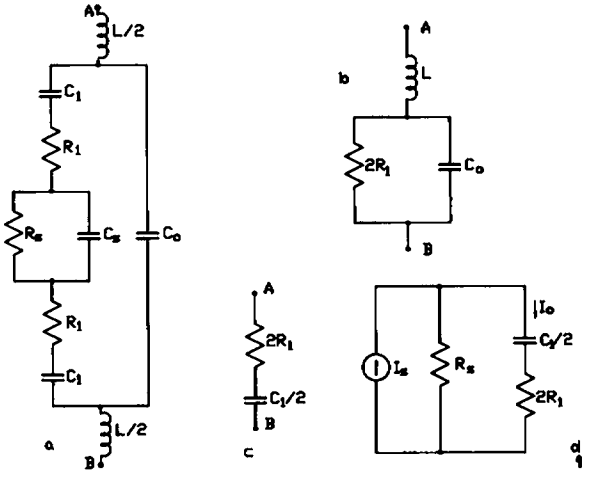

FIGURE 2. (*a*) The left portion of points A, B of the circuit in the Fig. 1 *a*, (*b*) The equivalent circuit of *a* in the 400 KHz to 100 MHz range. (*c*) The equivalent circuit of *a* in the 5 Hz to 100 Hz range. (*d*) The equivalent circuit of Fig. 1 *b* in the DC to 10 KHz range (see text).

of the impedance data based on the circuit of Fig. 2 *b* we determined that $C_o = 8.8 \pm 0.1$ pF and $L = 0.16 \pm 0.1$ μH and the values of R_l range from 75 Ω (100 mMKCl) through 700 Ω (10 mM KCl) to 6,500 Ω (1 mM).

C_l is the double layer capacitor formed between electrode and electrolyte solution. Since there is no electron exchange between the electrode and solution, C_l is the only pathway for the photocurrent to pass to the electrodes. The values of C_l and R_l are determined by measuring the impedance through points A and B from 5 Hz to 100 KHz under different salt concentrations. In this frequency range C_o can be considered as open (>2 MΩ) and L can be considered as a short (<0.02 Ω). So the remaining part of the circuit can be reduced to Fig. 2 *c*. Fitting the Bode magnitude and Bode phase plots of the impedance data by the circuit of Fig. 2 *c* we get $C_l = 11 \pm 1.5$ μF (1–100 mM KCl), increasing slightly with increasing salt concentration.

R_o is the input impedance of the I-V converter. Within the bandwidth of the *I-V* converter, this impedance can be represented as a resistor. R_o depend on the particular I-V converter used. (*a*) For signals in the nanosecond range, an I-V converter (model 313; Analog Modules Inc., Longwood, FL) with gain of 20 KV/A was used. This converter had been customized by the manufacturer as follows. The upper band limit −3dB frequency had been specially reduced to 100 MHz to be stable for an input capacitance in the range of 1 to 10 pF. The input was AC instead of DC coupled. The manufacturer reported a bandwidth of 750 Hz to 100 MHz and input impedance of 51 Ω from 1 MHz to 100 MHz. (*b*) For signals in the microsecond range, an I-V converter constructed with a OPA600BM op-amp (Burr-Brown Corp., Tucson, AZ) was used. It had gain of 10 KV/A and bandwidth of DC to 20 MHz. Because of the finite open loop voltage gain of the op-amps, the input impedance increased from 20 to 300 Ω as the frequency increased from 1 to 20 MHz. Since both R_s and R_l will be smaller than 300 Ω with high salt conditions, the high frequency portion of the photocurrent signal could be significantly changed by this frequency dependent input impedance of the I-V converter. Thus we only used this I-V converter for measurements in the μs range, although it has a bandwidth of 20 MHz when tested under high source impedance conditions. Over this range, R_o can be considered as zero. (*c*) For millisecond range measurements, an I-V converter made with Burr-Brown OPA102 op-amp was used. It has gain of 100 KV/A and bandwidth of DC to 700 kHz. To stay in the constant input impedance range, this I-V converter was used only for the measurements of signals that are slower than 1 ms.

The source resistance, R_s, is determined mainly by the electrolyte solution surrounding the membranes. R_s is very small compared with R_l because the distance across the membrane is much smaller than the distance between the membrane and the electrode. So, R_s will carry the largest portion of the I_s. C_s is the source capacitance determined by

the membranes and the surrounding electrolyte. We have not yet been able to determine accurate values of C_s and R_s, but the two most important roles that C_s and R_s play in the measurement of the photocurrent I_o can be discussed qualitatively.

The Time Constant of the Photocurrent. Since R_s is much smaller than the $2R_l + R_o$, from Fig. 1 *b* we can see that the time constant R_sC_s will set the limit for the fastest decaying kinetics that can be resolved. Increasing the ionic strength will reduce R_s and therefore reduce the time constant R_sC_s. Fig. 3 shows the first negative component of the photocurrent of purple membrane measured at several concentrations of KCl. The decay time constant of this component is limited by the time constant R_sC_s (see below). With increasing salt concentration, the time constant R_sC_s decreases. At 10 mM KCl, R_sC_s is ~60 ns and when the concentration of KCl increases to 1 M, the decay of first negative component becomes limited by the resolution of our digitizer. Then, a signal with a time constant (R_sC_s) of <32 ns is observed. We could also estimate C_s from this figure. At 10 mM KCl, R_s will be much, much $< R_l$ (700 Ω) and so we take its maximal value as 20 Ω. From the limit of the time constant, C_s will be larger than 3 nF.

The Amplitude of the Photocurrent. In the flat frequency response range of the measuring system, the ratio of measured current to the source current, I_o/I_s, is proportional to the ratio of $R_s/(R_s + 2R_l + R_o)$ or $R_s/(2R_l)$ to a first approximation (see below). A higher ratio of I_o/I_s means a larger signal or a better signal to noise ratio. This is especially important in measuring the small signal of the slowest photocurrent component. So, the error in estimating R_s will affect the prediction of the ratio of I_o/I_s at different ionic strengths. But the relation of signal amplitude to the salt concentration can be determined experimentally.

2. Frequency Response of the Measuring System

We first analyze the system as described, then modify it for optimized frequency response for several different experimental conditions. In order to analyze the frequency response of the system, we introduce the transfer function, $Tc(s)$, where s represents the frequency in the complex domain (see, for example, Aseltine, 1958). Since we are interested in the relationship of measured current $I_o(t)$ to the source current $I_s(t)$, we defined the transfer function as

$$Tc(s) = \frac{I_o(s)}{I_s(s)}, \qquad (1)$$

where, $I_o(s)$ and $I_s(s)$ are the Laplace transforms of $I_o(t)$ and $I_s(t)$. Our goal is to find and the frequency range in which $Tc(s)$ is constant and its phase shift is zero. Fig. 4 is the Bode plot of the transfer function simulated for the gel sample system (Fig. 1) in 10 mM KCl by PSPICE, a circuit analysis computer program modified from SPICE for personal computer use (MicroSim Corp., Laguna Hills, CA). Values of C_o, L, C_l, and R_l were those determined above. I_s is set equal to 1 unit for convenience. R_o is assumed to be 20 Ω, constant for the whole frequency range. R_s is assumed to be 10 Ω and C_s to be 6 nF to make the time constant R_sC_s equal to 60 ns as determined above from Fig. 3. The slope changes of log $Tc(f)$ and the phase shifts of $Tc(f)$ versus frequency indicate that $Tc(s)$ has 1 zero and 4 poles. Since the poles and zero are well separated, by varying the value of each component we can find the main factors that determine each zero and pole. The zero is at zero frequency. This means the system will not respond to a DC signal. The reason is that C_l is the only path for I_o (Fig. 1) so a DC signal could not pass C_l. Pole I is mainly determined by R_l and C_l. The corner frequency is

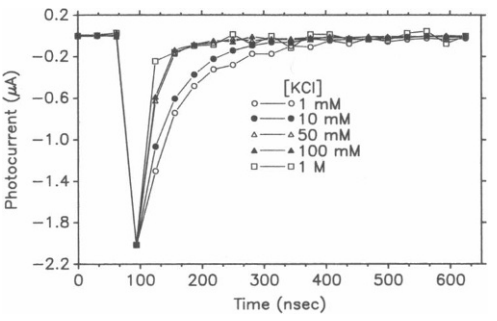

FIGURE 3. Photocurrent of the first negative component measured at different concentrations of KCl, 25°C, pH 6.0.

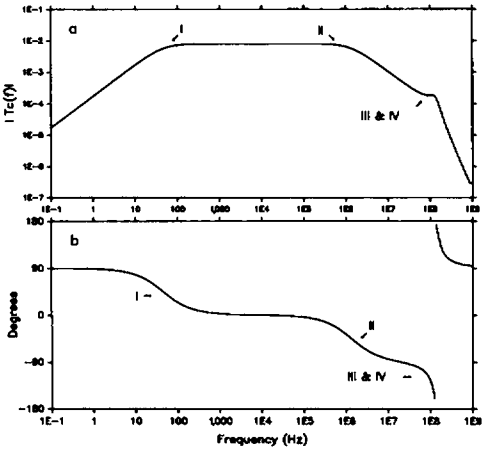

FIGURE 4. (*a*) Bode magnitude plot and (*b*) Bode phase plot of the transfer function calculated by the PSPICE circuit analysis computer program. 10 mM KCl condition is simulated. R_s is assumed to be 10Ω and C_s is assumed to be 6 nF to make the time constant R_sC_s equal to 60 ns (see text). R_o is 20 Ω.

$1/(2\pi R_1 C_1)$ Hz. Pole II is mainly determined by R_s and C_s and the corner frequency is at $1/(2\pi R_s C_s)$ Hz. III and IV are a pair of conjugated poles determined by C_o, L, and R_o. The corner frequency is at $1/(2\pi\sqrt{C_o L})$ Hz and the damping factor is equal to $R_o\sqrt{C_o}/(2\sqrt{L})$.

From Fig. 4 we can see that the measuring system described is accurate only for measurements in the 100 Hz to 1 MHz frequency range. In order to extend its flat frequency response range, the system must be modified.

A) Optimizing the Measuring System in the 10 KHz to 100 MHz Range. In this frequency range, there are three poles: II, III, and IV. For the system we initially tested, the corner frequency of poles III and IV is at 134 MHz and the frequency response bandwidth of the I-V converter is 750 Hz to 100 MHz. Reducing C_o and L will shift the corner frequency further from 100 MHz to make the I-V converter more stable and the system frequency response flatter. This was achieved by using two platinum wire electrodes of 0.7 mm in diameter, 18 mm in length and 8 mm apart and connecting them directly to the input pins of the I-V converter. C_o and L in this configuration are now found to be 6.3 pF and 0.05 μH respectively. The corner frequency under these conditions is shifted to 284 MHz. So, within the 100 KHz to 100 MHz range, only one pole is left. To shift this pole to higher frequencies, we must reduce C_s and R_s. Increasing the KCl concentration will reduce the R_s. It will also reduce the thickness of the double layer of ions surrounding the membrane which might lead to a change of C_s. As noted above, Fig. 3 shows the first, negative, phase of the photocurrent at different KCl concentrations measured with the improved system. We can see that with increasing ionic strength, the decay of this first component becomes faster. When the KCl is increased to 1 M, the half width of this negative phase is reduced to <32 ns, limited by the resolution of our transient digitizer. Fig. 3 indicates that for KCl concentrations in the millimolar range, kinetic studies of the decay of the fast negative component of the photocurrent are limited by the time constant, R_sC_s. At 10 mM KCl, we are only able to study the kinetics of photo processes which are longer than 60 ns. When the KCl is increased up to 1 M, we are able to study kinetics longer than 32 ns, limited by the resolution of the digitizer and the exciting laser.

Fig. 5 *a* is the photocurrent response showing both the fast negative phase and the slower positive phase measured with our improved system in 100 mM KCl. To get a clear view of the rising phase of the positive component, Fig. 5 *b* shows the temperature dependence of this component on an expanded scale while Fig. 5 *c* shows the temperature dependence of the K to L transition, measured at 660 nm, for comparison. The Arrhenius plots of their rate constants are shown in Fig. 5 *d*. We can see that the rising positive phase of the photocurrent is closely correlated with the formation of the L intermediate. Our optimized system has clearly separated this component from the RCs of the measuring system at room temperature or even higher (35°C). It should be noted that both the K-L and L-M transitions could produce a photocurrent phase which have the same rate constant as the K-L optical transition. However, since this rising phase changed the polarity from negative to positive, we conclude that it is produced by both K-L and L-M transition. The K-L transition produces a very small photocurrent in the negative direction as suggested by Keszthelyi et al. (1980), while L-M transition produces a photocurrent in the positive direction.

B) Optimizing the Measuring System for the DC to 10 KHz Range. In this frequency range C_s can be taken as an open circuit because the impedance of C_s is much larger than the impedance of R_s. L and R_o can be looked on as short circuits because their impedances are much smaller (<1 Ω) than the impedance of C_o or R_1. Therefore the circuit of Fig. 1 *b* can be simplified to Fig.

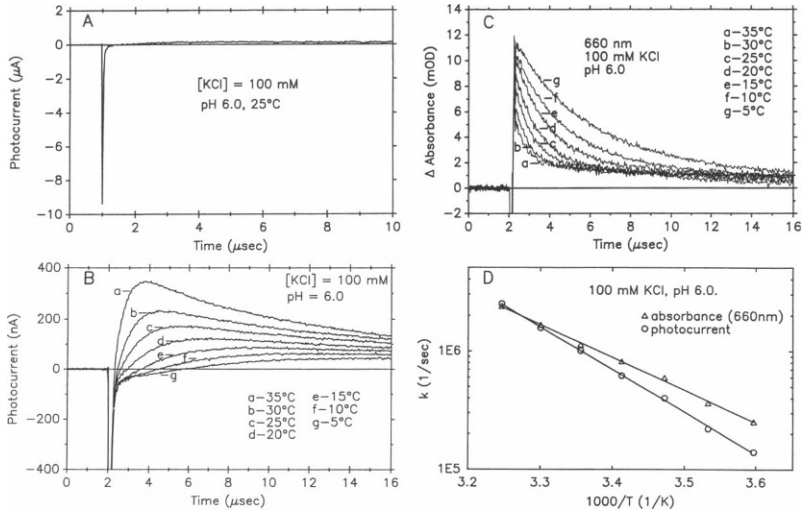

FIGURE 5 Photocurrent and absorbance kinetics measured with our improved system. (*a*) Photocurrent trace showing both the fast negative phase and the slower positive phase. (*b*) The temperature dependence of the rising phase of the positive photocurrent component on an expanded scale. (*c*) The temperature dependence of the optical K to L transition. (*d*) Arrhenius plots of the rate constants of the rising phase of the photocurrent (E_a = 16.4 kcal/mol, $A = 1.15 \times 10^{18} s^{-1}$) and K to L absorbance transition (E_a = 12.7 kcal/mol, $A = 2.4 \times 10^{15} s^{-1}$).

2 d. Using Ohm's law, we get

$$T_c(s) = \frac{I_o}{I_s} = \frac{R_s}{R_s + 2R_1} \cdot \frac{S}{\frac{2}{(R_s + 2R_1)C_1} + S} = B \cdot \frac{S}{\frac{1}{\tau_o} + S}, \quad (2)$$

where $B = R_s/(R_s + 2R_1)$, $\tau_o = (R_s + 2R_1)C_1/2 \cong R_1C_1$. From Eq. 2 we can see that in this frequency range there is 1 pole at $f = 1/(2\pi R_1C_1)$ Hz and 1 zero at $f = 0$ Hz just as for the conclusions derived by using PSPICE for the entire frequency range. To see how I_s will be affected by this system in the time domain, let us assume the signal has the form $I_s(t) = Ae^{-t/\tau}$ where A is a constant and τ is rate of decay of the signal. By Laplace transform we get

$$I_s(s) = \frac{A}{1/\tau + S} \quad (3)$$

So

$$I_o(s) = I_s(s) \cdot Tc(s) = A \cdot B \frac{S}{(1/\tau_o + S) \cdot (1/\tau + S)}. \quad (4)$$

By inverse Laplace transform, we get

$$I_o(t) = A \cdot \frac{R_s}{R_s + 2R_1} \cdot \left(\frac{\tau_o}{\tau_o - \tau} e^{-t/\tau} + \frac{\tau}{\tau - \tau_o} e^{-t/\tau_o} \right). \quad (5)$$

Fig. 6 shows the plot of $I_o(t)$ with different time constants, τ. From Fig. 6 we can see that only when $\tau \leq 0.1\ \tau_o$, will I_o have a shape very similar to I_s. When $\tau = \tau_o$, the signal will be significantly distorted. And when $\tau \gg \tau_o$, I_o will be an exponential with a time constant, τ_o.

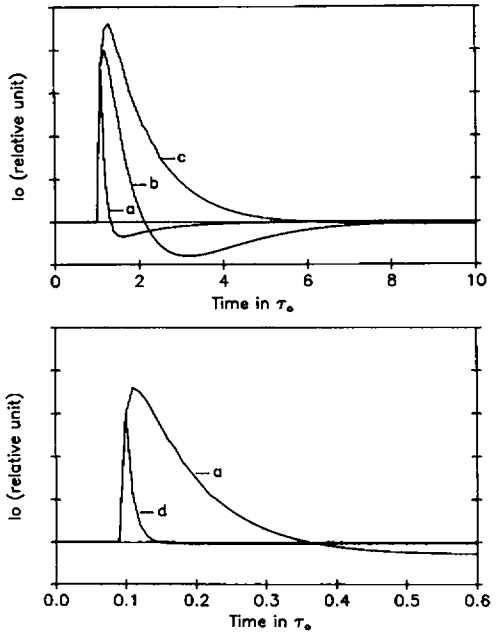

FIGURE 6. Simulated transient response of the circuit of Fig. 2 d to an exponential input current, $I_s(t) = Ae^{-t/\tau}$, with different values of the time constant, τ. $\tau_o = R_1C_1$. Curve a, $\tau = 0.1\ \tau_o$; curve b, $\tau = \tau_o$; c, $\tau = 100\ \tau_o$ and curve d, $\tau = 0.01\ \tau_o$; respectively.

The time constant, R_1C_1, of the electrode tested at 10 mM KCl is ~8 ms. So only an exponential signal $I_s(t)$ with a lifetime shorter than 0.8 ms could be measured without much distortion. In order to make the system able to detect slower signals, we must shift the pole to as low a frequency as possible to cancel the zero. One way to do this is to increase R_1 by lowering the ionic strength. But this will reduce the amplitude of the signal. And since the ms component of the photocurrent is already much smaller than the faster components, this change would increase the difficulty of the measurement. So, the best way to increase R_1C_1 is to increase C_1. Platinizing the platinum electrode, which increases the surface area of the electrode by more than 100 times, will increase C_1 by about a factor of 100. At 50 mM KCl, C_1 of the platinized electrode was found to be ~1,000 μF, compared with 12 μF for the unplatinized electrodes. At lower ionic strengths, we could not detect C_1 due to limitations of measuring instrument but the impedance is flat to at least 5 Hz. Since C_1 has only a slight dependance on the ionic strength in this range, we can assume C_1 for 10 mM KCl is ~1,000 μF also. That means by using platinized electrodes and by keeping R_1 larger than 700 Ω (for KCl $\leq$ 10 mM), the time constant of R_1C_1 will be >700 ms. Thus, the kinetics of a photocurrent with a lifetime ~70 ms will not be distorted by this measuring system. The photocurrent measured with the original smooth surface platinum electrodes and platinized platinum electrodes at 1 and 10 mM KCl are shown in Fig. 7 a and b. The absorption change at 400 nm due to the M intermediate is also shown in Fig. 7 c. Because the difference in the kinetics of M decay at 1 mM and 10 mM KCl is small, only the kinetics of M decay at 10 mM KCl are shown. From Fig. 7 we can see that the amplitude and the shape of the photocurrent measured with unplatinized electrodes change with the ionic strength, as analyzed above. However, a change of salt concentration does not cause a change in the photocurrent waveform when measured with platinized electrodes, indicating that the measuring system is working accurately. It also shows that with the optimized conditions, i.e., 10 mM KCl (or $R_1 \approx 700\ \Omega$) and platinized electrodes, the absorption changes associated with the M intermediate have similar kinetics as the slow component of the photocurrent (12.1 and 10.4 ms, respectively), supporting the assumption that this component of the photocurrent is related to the M intermediate (Keszthelyi et al., 1980).

The integration of $I_s(t)$ from time zero to infinity will be total charge transferred, which is the product of the number of charges moved and the distance the charges moved during the transitions of the photointermediates. But the integration of $I_o(t)$ in Eq. 5 from time zero to infinity is zero because there is a capacitor, C_1, in series in the circuit. This series capacitor is the only path for the

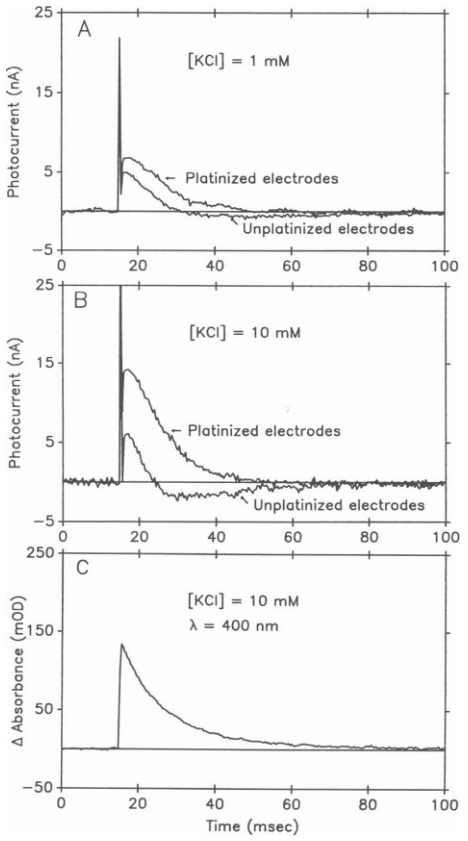

FIGURE 7 A comparison of the photocurrent and the absorbance change associated with the *M* intermediate, measured in the ms range with platinized and unplatinized electrodes, 25°C, and pH 6.0. (*a*) Photocurrent response measured in 1 mM KCl. (*b*) Photocurrent response measured in 10 mM KCl. (*c*) Optical measurement of intermediate in 10 mM KCl monitored at 400 nm.

current and so any component that initially passes through C_l will also be discharged through C_l with a time constant of $(R_s + 2R_l + R_o)C_l/2$. Theoretically, the integral of the photocurrent through the I-V converter, I_o, will always be zero (except the charge left on C_l) no matter how many net protons or other ions have been pumped across the purple membrane. When $\tau \ll \tau_o$, the discharging current will be very small and may not be easily detected. So, when using the integration of photocurrent with time to study light induced charge movements in bacteriorhodopsin, care must be taken to make sure that the $\tau \ll \tau_o$ condition obtains and with the understanding that the discharging current of C_l is omitted. When multiple components are involved, the discharging current of a fast component may be incorrectly interpreted as the photo current of a slower component.

DISCUSSION

Many different preparation and measurement systems have been used to study the photoelectric activity of purple membranes. A great advantage of the electric field oriented preparation is that enough material is present so that light induced absorption changes as well as the photoelectric signals can be measured under same conditions. Moreover, one does not have the possible distortion of the intrinsic waveform of the pigment's photoelectric response by the *RC* constant of any thin membrane that the pigment might be attached to. For measuring the photocurrent with a thin membrane preparation, R_s is much larger than $R_o + 2R_l$ and therefore, the time constant $(R_o + 2R_l)C_s$ will limit the time resolution to ~3–5 μs (Fahr et al., 1981; Huebner et al., 1984), much slower than we can get from an electric field oriented sample. Of the electric field oriented sample systems, the gel preparation is probably the best available for photocurrent measurements because: (*a*) Since the measurements can be made at high salt concentrations, it is possible to study the kinetics of the purple membrane photocurrent in the nanosecond range. From a microscopic point of view, we can consider that it is the small value of R_s rather than the I-V converter that clamps the voltage across the C_s of each purple membrane fragment and made the fast photocurrent measurement possible. (*b*) When using an electric field to orient purple membrane in a solution, the absorption of the purple membrane onto a platinized electrode is a major difficulty, while for gel samples, the electrode is not touching the purple membranes. Therefore the electrode can be platinized to increase C_l, allowing the accurate study of the kinetics in the millisecond range. (*c*) a constant orientation of purple membrane can be maintained while pH and ionic strength are changed.

As the work of others (e.g., Trissl et al. [1984]; Hong and et al. [1976]) have shown, it is imperative to determine the circuit characteristics and limitations of photoelectric signal measurements. The aim of this report is the characterization of our photocurrent measuring device and the adjustments necessary to the initial circuit so that a flat frequency response is obtained over the needed frequency range.

From the above experiments we can see that for the millisecond range measurements, special care must be taken to control the time constant R_lC_l. If the electrode is not platinized, increasing the ionic strength may shorten the apparent lifetime of the millisecond component; when the life time of $I_s(t)$ slows down, $I_o(t)$ will reach a limit of the time constant R_lC_l. Thus using platinized electrodes and keeping R_l high (>700 Ω) by adjusting the ionic strength are essential for accurate photocurrent measurements in the millisecond range. For studying photocurrent components that have lifetimes longer than 70 ms, a further increase in R_lC_l will be necessary. This might be accomplished by increasing C_l by using platinized platinum electrodes made from a sheet instead of wire electrodes or by increasing R_l by reducing the ionic strength further. Increasing R_o instead of R_l, as was used by Dér et al. (1985) (100 KΩ), is another alternative for the ms range measurements when a higher salt concentration is necessary. But this will reduce the signal amplitude and is not good for ns range measurements. Using reversible elec-

trodes such as Ag/AgCl electrodes instead of platinum electrodes is also a possible solution. In the low frequency range, the Ag/AgCl electrode will form a resistive coupling between the electrolyte solution and the I-V converter, making it possible to measure a DC photocurrent signal. But, care must be taken because of the rate limitation of the electrochemical reaction on the Ag/AgCl electrode, the coupling between the electrolyte solution and the I-V converter will change from resistive to capacitive with increasing frequency. In other words, using reversible electrodes will shift the zero from frequency zero to a higher frequency, making the DC measurement possible, but it will also make the higher frequency measurements more complicated.

For measurements in the microsecond range, all the capacitors and inductors in the equivalent circuit could be eliminated because they could either be looked on as open or as shorts. The frequency response of the transfer function is flat for most ionic strengths even using platinum wire electrodes. This may be why most of published photocurrent measurements are fairly consistent with each other in this time range and also correlate with the optical L to M transition (e.g., Dér et al., 1985, Hristova et al., 1986).

For the nanosecond range, special care must be paid to the I-V converter because this wideband I-V converter could be looked on as a very high gain voltage amplifier. Removing the poles III and IV (Fig. 4) far from the frequency response range is very important for stability. Of the factors that determine poles III and IV, L, the inductance of the electrodes and wires, is the key factor. Therefore, shortening the electrodes and wire to the minimum to reduce L is imperative. From the I-V converter point of view, the source resistor is equal to $2R_1$, which, unlike a usual current source, has a very low value, sometimes as low as 200 Ω when a high salt concentration is used. Thus, the I-V converter must have two special requirements: (*a*) a low and constant input impedance. This is especially important for an I-V converter made of op-amps because the finite open-loop voltage gain in that frequency range. (*b*) not only low current noise but also low voltage noise and very good grounding. Otherwise the noise at the grounded input point will be amplified by a factor of $(Z_f + 2R_1)/2R_1$ which could be as large as 1,000 at high salt conditions.

The 10 ns to 1 μs range is the most confusing range for photoelectric measurements of the electric field oriented sample system. Signals incorrectly looking like they are composed of more than one exponential could be induced by the measuring system because: (*a*) The discharge of C_s has a life time, R_sC_s, in this range. (*b*) Most current amplifiers have their response time in this range. Since most amplifiers are second order systems, their response can be fit by more than one exponential (see, for example, Sigworth, 1983. (*c*) For photovoltage measurements, the conjugated poles III and IV of Fig. 4 will change to a single pole with a corner frequency of $1/(2\pi C_o[2R_1//R_o])$ because R_o is much higher than with photocurrent measuring conditions. This pole will correspond to a exponential in the time domain with a life time of $C_o(2R_1//R_o)$, which will also fall into this range in most cases. In our optimized photocurrent measuring system, only one exponential introduced by the measuring system, with time constant R_sC_s, is left. We have minimized this time constant to <32 ns, and therefore there is no distortion by the measuring system for signals slower than this. As shown in Fig. 5, we could clearly identify the rising phase of the component related to the L intermediate at 35°C without distortion by the RCs of the measuring system.

Finally, it should be mentioned that the photoelectric signal of purple membrane could also be capacitively coupled with the electrodes. In other words, there is a small capacitor in parallel with C_1 and R_1. This small capacitor could bypass a high frequency signal if its impedance were comparable with the impedance of R_1. But since the distance between the electrode and gel is ~1.5 mm and the geometry of the electrode is a wire, this capacitor is very small. Its value is estimated to be <0.3 pF (tested under very low conductivity conditions and a high input impedance amplifier). For photocurrent measurements in 1 mM to 1M salt, this small capacitance will not affect the shape of the signal because its impedance is >50 kΩ at 10 MHz. So, we did not include it in the Fig. 1. However, if the measuring system uses sheet electrodes, very low conductivity conditions, or solution instead of gel samples, this capacitive coupling will be important for high frequency signals.

We would like to thank D. DeVault, L. R. Faulkner, B. Oakley, P. Ormos, and L. Keszthelyi for helpful discussions, and H. Djellab and J. Gooch for generously helping with the impedance measurements.

This work was supported by Department of Energy grant DEAC02-82ER12087 and NSF grant DBM 85-15339.

Received for publication 27 November 1987 and in final form 21 March 1988.

REFERENCES

Aseltine, J. A. 1958. Transform method in linear system analysis. McGraw-Hill, New York.

Becher, B., and J. Y. Cassim. 1975. Improved isolation procedures for the purple membrane of *Halobacterium halobium*. *Prep. Biochem.* 5:161–178.

Dancsházy, Z., R. Govindjee, B. Nelson, and T. G. Ebrey. 1986. A new intermediate in the photocycle of bacteriorhodopsin. *FEBS (Fed. Eur. Biochem. Soc.) Lett.* 209:44–48.

Dér, A., P. Hargittai, and J. Simon. 1985. Time-resolved photoelectric and absorption signals from oriented purple membranes immobilized in gel. *J. Biochem. Biophys. Methods.* 10:259–300.

Drachev, L. A., A. D. Kaulen, and V. P. Skulachev. 1978. Time resolution of the intermediate steps in the bacteriorhodopsin-linked electrogenesis. *FEBS (Fed. Eur. Biochem. Soc.) Lett.* 87:161–167.

Fahr, A., P. Läuger, and E. Bamberg. 1981. Photocurrent kinetics of purple-membrane sheets bound to planar bilayer membranes. *J. Membr. Biol.* 60: 50–62.

Groma, G. I., G. Szabó, and Gy. Váró. 1984. Direct measurement of picosecond charge separation in bacteriorhodopsin. *Nature (Lond.)*. 308:557–558.

Herrmann, T. R., and G. W. Rayfield. 1978. The electrical response to light of bacteriorhodopsin in planar membranes. *Biophys. J* 21:111–125.

Hong, F. T., and D. Mauzerall. 1976. Tunable voltage clamp method: application to photoelectric effects in pigmented bilayer lipid membranes. *J. Electrochem. Soc.* 123:1317–1324.

Hristova, S. G., A. Dér, Gy. Váró, and L. Keszthelyi. 1986. Effect of pH on the photocycle and electric signal kinetics in purple membrane subjected to digestion with proteolytic enzymes. *Photobiochem. Photobiophys.* 12:231–241.

Huebner, J. S., R. T. Arrieta, I. C. Arrieta, and P. M. Pachori. 1984. Photo-electric effects in bilayer membranes; electrometers and voltage clamps compared. *Photochem. Photobiol.* 39:191–198.

Keszthelyi, L. 1984. Intramolecular charge shifts during the photoreaction cycle of bacteriorhodopsin. *In* Information and Energy Transduction in Biological Membranes. Bolis, C. L. et al. editors. 55–71. Alan R. Liss, New York.

Keszthelyi, L., and P. Ormos. 1980. Electric signals associated with the photocycle of bacteriorhodopsin. *FEBS (Fed. Eur. Biochem. Soc.) Lett.* 109:189–193.

Keszthelyi, L., and P. Ormos. 1983. Displacement current on purple membrane fragments oriented in a suspension. *Biophys. Chem.* 18:397–405.

Liu, S., T. Ebrey, J. Zingoni, R. Crouch, J. -M. Fang, and K. Nakanishi. 1987. Fast photoelectric response from artificial pigments of bacteriorhodopsin. *Biophys. J.* 51:134*a*. (Abstr.)

Ormos, P., S. Hristova, and L. Keszthelyi. 1985. The effect of pH on proton transport by bacteriorhodopsin. *Biochim. Biophys. Acta.* 809:181–186.

Sigworth, F. J. 1983. Electronic design of the patch clamp. *In* Single channel recording. B. Sakmann and E. Neher, editors. Plenum Publishing Co., New York.

Trissl, H. -W. 1983. Charge displacements in purple membranes adsorbed to a heptane/water interface. Evidence for a primary charge separation in bacteriorhodopsin. *Biochim. Biophys. Acta.* 723:327–331.

Trissl, H. -W. 1985. I. Primary electrogenic processes in bacteriorhodopsin probed by photoelectric measurements with capacitative metal electrodes. *Biochim. Biophys. Acta.* 806:124–135.

Trissl, H. -W., A. Dér, P. Ormos, and L. Keszthelyi. 1984. Influence of stray capacitance and sample resistance on the kinetics of fast photovoltages from oriented purple membranes. *Biochim. Biophys. Acta.* 765:288–294.

Trissl, H. -W., and W. Gärtner. 1987. Rapid charge separation and bathochromic absorption shift of flash-excited bacteriorhodopsins containing 13-cis or all-trans forms of substituted retinals. *Biochemistry.* 26:751–757.

Trissl, H. -W., and M. Montal. 1977. Electrical demonstration of rapid light-induced conformational changes in bacteriorhodopsin. *Nature (Lond.)*. 266:655–657.

Váró, G. 1981. Dried oriented purple membrane samples. *Acta Biol. Acad. Sci. Hung.* 32:301–310.